Germanium-on-Glass solar cells: fabrication and characterization

Vito Sorianello,[1] Lorenzo Colace,[1,*] Carlo Maragliano,[1] Dominic Fulgoni,[2] Lee Nash,[2] and Gaetano Assanto[1]

[1]*NooEL- Nonlinear Optics and OptoElectronics Lab, University "Roma Tre," Via della Vasca Navale 84, 00146 Rome, Italy*

[2]*Circadian Solar, One Sovereign Court, Sir William Lyons Road, Coventry CV4 7EZ, United Kingdom*

**colace@uniroma3.it*

Abstract: We report on Germanium on Glass solar cells realized by wafer bonding, layer splitting and epitaxial regrowth. We provide a detailed description of the layer transfer process and discuss the material characterization. The solar cells are fabricated and tested to extract the most significant figures of merit, evaluating their performance versus device area and operating temperature. The cells exhibit typical conversion efficiencies exceeding 2.4% under AM1.5 irradiation and a maximum efficiency of 3.7% under concentrated excitation. This Germanium on Glass approach is promising in terms of added flexibility in multi-junction engineering and allows a significant cost reduction thanks to the re-usability of the Ge substrates.

©2013 Optical Society of America

OCIS codes: (040.5350) Photovoltaic; (160.6000) Semiconductor materials; (310.3840) Materials and process characterization.

References and links

1. N. Mason, "Manufacturing technology: fabrication innovations," Nat. Photonics **2**(5), 281–283 (2008).
2. S. Kurtz, "Opportunities and challenges for development of a mature concentrating photovoltaic power industry," *NREL Techn. Report*, No. 520-43208 (2009).
3. R. R. King, A. Boca, W. Hong, X.-Q. Liu, D. Bhusari, D. Larrabee, K. M. Edmondson, D. C. Law, C. M. Fetzer, S. Mesropian, and N. H. Karam, "Band-gap-engineered architectures for high-efficiency multijunction concentrator solar cells," in *Proc. 24th European Photovoltaic Solar Energy Conf.*, Sep. 2009, pp. 55–61.
4. D. C. Law, R. R. King, H. Yoon, M. J. Archer, A. Boca, C. M. Fetzer, S. Mesropian, T. Isshiki, M. Haddad, K. M. Edmondson, D. Bushari, J. Yen, R. A. Sherif, H. A. Atwater, and N. H. Karam, "Future technology pathways of terrestrial III-V multijunction solar cells for concentrator photovoltaic systems," Sol. Energy Mater. Sol. Cells **94**(8), 1314–1318 (2010).
5. J. F. Geisz, D. J. Friedman, J. S. Ward, A. Duda, W. J. Olavarria, T. E. Moriarty, J. T. Kiehl, M. J. Romero, A. G. Norman, and K. M. Jones, "40.8% efficient inverted triple-junction solar cell with two independently metamorphic junctions," Appl. Phys. Lett. **93**(12), 123505 (2008).
6. C. D. Law, D. M. Bhusari, S. Mesropian, J. C. Boisvert, W. D. Hong, A. Boca, D. C. Larrabee, C. M. Fetzer, R. R. King, and N. H. Karam, "Semiconductor-bonded III-V multijunction space solar cells," in *Proc. 34th IEEE Photovoltaic Specialists Conference*, Jun. 2009, pp. 2237–2239.
7. M. Konagai, M. Sugimoto, and K. Takahashi, "High efficiency GaAs thin film solar cells by peeled film technology," J. Cryst. Growth **45**, 277–280 (1978).
8. E. Yablonovitch, T. Gmitter, J. P. Harbison, and R. Bhat, "Extreme selectivity in the lift-off of epitaxial GaAs films," Appl. Phys. Lett. **51**(26), 2222–2224 (1987).
9. P. Demeester, I. Pollentier, P. D. Dobbelaere, C. Brys, and P. V. Daele, "Epitaxial lift-off and its applications," Semicond. Sci. Technol. **8**(6), 1124–1135 (1993).
10. W. P. Maszara, G. Goetz, A. Caviglia, and J. B. McKitterick, "Bonding of silicon wafers for silicon-on-insulator," J. Appl. Phys. **64**(10), 4943–4950 (1988).
11. H. Taguchi, T. Soga, and T. Jimbo, "Epitaxial lift-off process for GaAs solar cell on Si substrate," Sol. Energy Mater. Sol. Cells **85**, 85–89 (2005).
12. J. M. Zahler, K. Tanabe, C. Ladous, T. Pinnington, F. D. Newman, and H. Atwater, "High efficiency InGaAs solar cells on Si by InP layer transfer," Appl. Phys. Lett. **91**(1), 012108 (2007).
13. K. Lee, K. Shiu, J. D. Zimmerman, C. K. Renshaw, and S. R. Forrest, "Multiple growths of epitaxial lift-off solar cells from a single InP substrate," Appl. Phys. Lett. **97**(10), 101107 (2010).
14. T. Takamoto, T. Agui, A. Yoshida, K. Nakaido, H. Juso, K. Sasaki, K. Nakamora, H. Yamaguchi, T. Kodama, H. Washio, M. Imaizumi, and M. Takahashi, "World's highest efficiency triple-junction solar cells fabricated by

#179572 - $15.00 USD Received 8 Nov 2012; revised 21 Dec 2012; accepted 9 Jan 2013; published 10 Jan 2013

inverted layers transfer process," in *Proc. 35th IEEE Photovoltaic Specialists Conference*, Jun. 2010, pp. 412–417.
15. J. Boisvert, D. Law, R. King, D. Bhusari, X. Liu, A. Zakaria, W. Hong, S. Mesropian, D. Larrabee, R. Woo, A. Boca, K. Edmondson, D. Krut, D. Peterson, K. Rouhani, B. Benedikt, and N. H. Karam, "Development of advanced space solar cells at Spectrolab," in *Proc. 35th IEEE Photovoltaic Specialists Conference*, Jun. 2010, pp. 123–127.
16. D. D. Krut, B. T. Cavicchi, and D. R. Lillington, "The development of Ge bottom cell for monolithic and stacked multi-junction applications," in *Proc. 22nd IEEE Photovoltaic Specialists Conference*, Oct. 1991, pp. 90–92.
17. B. Bitnar, "Silicon, germanium and silicon/germanium photocells for thermophotovoltaics applications," Semicond. Sci. Technol. **18**(5), S221–S227 (2003).
18. L. D. Partain, M. S. Kuryla, R. E. Weiss, R. A. Ransom, P. S. McLeod, L. M. Fraas, and J. A. Cape, "26.1% solar cell efficiency for Ge mechanically stacked under GaAs," J. Appl. Phys. **62**(7), 3010–3015 (1987).
19. N. E. Posthuma, J. Van der Heide, G. Flamand, and J. Poortmans, "Emitter formation and contact realization by diffusion for germanium photovoltaic devices," IEEE Trans. Electron. Dev. **54**(5), 1210–1215 (2007).
20. R. Ginige, B. Corbett, M. Modreanu, C. Barrett, J. Hilgarth, G. Isella, D. Chrastina, and H. von Känel, "Characterization of Ge-on-Si virtual substrates and single junction GaAs solar cells," Semicond. Sci. Technol. **21**(6), 775–780 (2006).
21. R. B. Bergmann, T. J. Rinke, T. A. Wagner, and J. H. Werner, "Thin film solar cells on glass based on the transfer of monocrystalline Si films," Sol. Energy Mater. Sol. Cells **65**(1-4), 355–361 (2001).
22. X. Y. Lee, A. K. Verma, C. Q. Wu, M. Goertemiller, E. Yablonovitch, J. Eldredge, and D. Lillington, "Thin film GaAs solar cells on glass substrates by epitaxial liftoff," in *Proc. 25th IEEE Photovol. Spec. Conf.*, Washington D.C., May 13–17, 1996, pp. 53–55.
23. Y. Yazawa, K. Tamura, S. Watahiki, T. Kitatani, J. Minemura, and T. Warabisako, "GaInP single-junction and GaInP/GaAs two-junction thin-film solar cell structures by epitaxial lift-off," Sol. Energy Mater. Sol. Cells **50**(1-4), 229–235 (1998).
24. J. M. Zahler, C. G. Ahn, S. Zaghi, H. A. Atwater, C. Chu, and P. Iles, "Ge layer transfer to Si for photovoltaic applications," Thin Solid Films **403-404**, 558–562 (2002).
25. M. J. Archer, D. C. Law, S. Mesropian, M. Haddad, C. M. Fetzer, A. C. Ackerman, C. Ladous, R. R. King, and H. A. Atwater, "GaInP/GaAs dual junction solar cells on Ge/Si epitaxial templates," Appl. Phys. Lett. **92**(10), 103503 (2008).
26. G. Taraschi, A. J. Pitera, and E. A. Fitzgerald, "Strained Si, SiGe, and Ge on-insulator: review of wafer bonding fabrication techniques," Solid-State Electron. **48**(8), 1297–1305 (2004).
27. L. Chen, P. Dong, and M. Lipson, "High performance germanium photodetectors integrated on submicron silicon waveguides by low temperature wafer bonding," Opt. Express **16**(15), 11513–11518 (2008).
28. L. Colace, V. Sorianello, G. Assanto, D. Fulgoni, L. Nash, and M. Palmer, "Germanium on Glass: a novel platform for light sensing devices," IEEE Photonics J. **2**(5), 686–695 (2010).
29. Y. Chao, R. Scholz, M. Reiche, U. Gösele, and J. C. Woo, "Characteristics of germanium-on-insulators fabricated by wafer bonding and hydrogen-induced layer splitting," Jpn. J. Appl. Phys. **45**(11), 8565–8570 (2006).
30. H. Min, Y. Joo, and O. Song, "Effects of wafer cleaning and annealing on glass/silicon wafer direct bonding," J. Electron. Packag. **126**(1), 120–123 (2004).
31. A. Plößl and G. Krauter, "Wafer direct bonding: tailoring adhesion between brittle materials," Mater. Sci. Eng. **25**(1-2), 1–88 (1999).
32. R. People, "Physics and applications of Ge_xSi_{1-x}/Si strained-layer heterostructures," IEEE J. Quantum Electron. **22**(9), 1696–1710 (1986).
33. C. L. Andre, D. M. Wilt, A. J. Pitera, M. L. Lee, E. A. Fitzgerald, and S. A. Ringel, "Impact of dislocation densities on n^+/p and p^+/n junction GaAs diodes and solar cells on SiGe virtual substrates," J. Appl. Phys. **98**(1), 014502 (2005).
34. S. P. Philipps, W. Guter, E. Welser, J. Schöne, M. Steiner, F. Dimroth, and A.W. Bett, *Present Status in the Development of III–V Multi-Junction Solar Cells* (Springer, 2012), Chap. 1.
35. D. P. Malta, J. B. Posthill, R. J. Markunas, and T. P. Humphreys, "Low defect density germanium on silicon obtained by a novel growth phenomenon," Appl. Phys. Lett. **60**(7), 844–846 (1992).
36. G. Masini, L. Colace, F. Galluzzi, and G. Assanto, "Advances in the field of poly-Ge on Si near infrared photodetectors," Mater. Sci. Eng. B **69-70**, 257–260 (2000).
37. W. C. Dash and R. Newman, "Intrinsic optical absorption in single-crystal germanium and silicon at 77°K and 300°K," Phys. Rev. **99**(4), 1151–1155 (1955).
38. M. A. Green, *Solar Cells* (Prentice-Hall, 1982).

1. Introduction

Despite the large annual growth of the photovoltaic industry, higher than 30%/year in the last decade, even in leading countries a rather small fraction of the consumed electric energy is derived from the sun [1]. The reason is fundamentally tied to the higher cost of solar kWh with respect to traditional sources. New approaches and technologies are emerging, all aimed at the reduction of fabrication costs and/or the increase of conversion efficiency, which has a direct impact on the energy price in $/kWh [2]. While the present solar cell production is

#179572 - $15.00 USD Received 8 Nov 2012; revised 21 Dec 2012; accepted 9 Jan 2013; published 10 Jan 2013
(C) 2013 OSA

strongly dominated (90%) by the mature silicon technology, significant progress has been made by employing viable alternatives, including thin film and multijunction technologies. Multi-junction (MJ) solar cells based on III-V semiconductors are the most efficient photovoltaic converters with a demonstrated 41.6% record efficiency [3] and have the greatest potential for improvements with efficiencies theoretically exceeding 60% [4].

Unfortunately, semiconductors with optimal band-gaps (for the effective partition of the solar spectrum) are not lattice-matched; hence, tradeoffs between gap and crystalline quality are required, since gap tuning increases lattice mismatch thus introducing defects. Today, high conversion MJ solar cells are based on two approaches: *lattice-matched* and the more recent *metamorphic* cells. In the latter, thin relaxed electrically inactive buffer layers help manage the strain and allow the fabrication of three-junction structures with relatively large lattice-mismatches and efficiencies exceeding 40% [3,5]. Nevertheless, in order to fully exploit the potentials of 4-, 5- and 6- junction cells, new technological pathways are needed to provide more design flexibility and ensure higher and higher energy yields, to be accomplished by a combination of different techniques such as metamorphic, inverted crystal growth, bi-facial epigrowth and layer-transfer, the latter (or suitable templates) grown on their native substrate and then exfoliated and placed on the stack [6].

Since MJ technologies have great potential but increase the fabrication cost because of the expensive materials (especially the substrate) and the low process yields, layer transfer is viable inasmuch as it improves design flexibility (allowing the use of optimum gap semiconductors regardless of the lattice mismatch) and lowers costs via volume-effective usage of (expensive) substrates. Wafer bonding was first introduced by Konagai *et al.* for realizing thin film GaAs on cheap substrates [7], later adopted by other investigators in order to overcome the problems of heteroepitaxy with lattice mismatched crystals [8,9] and widely employed in Silicon on Insulator technology [10]. Then, several groups undertook the fabrication of thin film solar cells by layer transfer using GaAs on Si [11], InGaAs on Si [12] or flexible substrates [13], all aiming at lowering the costs of compound cells relative to those grown on bulk substrates. Very recently, wafer bonding was used in MJ technology to transfer epitaxially grown III-V layers (or part of them) from GaAs (or Ge) to a (cheaper) handling substrate [14,15].

Germanium is an important material for photovoltaic applications. Nowadays, high-performance devices and future roadmaps comprise cells with a Ge bottom-layer for the collection of the infrared portion of the solar spectrum, contributing with a 4% to 6% extra efficiency conversion [16]. Besides their role as the most common bottom element of MJs, Ge solar cells as stand-alone devices are also attractive for thermophotovoltaic applications [17] as well as mechanically stacked MJ [18]. A 7.8% record energy conversion efficiency of stand-alone Ge solar cells was demonstrated using diffused Ge substrates [19].

Since high quality Ge substrates weigh considerably on the overall cost [20], the transfer of the Ge cell onto a cheaper substrate such as glass is more than intriguing. Fabricating solar cells on glass by layer transfer has been proposed for various semiconductors including Si [21], GaAs [22] and GaInP/GaAs tandem [23]. Ge bonding on Si or SiO_2 was attempted for several applications, from photovoltaics [24,25] to electronics [26] and to photonics [27]. The transfer of Ge on glass substrates in order to obtain high quality Ge films towards near infrared photodetectors and bottom-element solar cells was recently attempted by us [28].

In this work, we fabricated and compared Ge-on-Glass cells (GoG) and reference Ge-on-Ge cells, evaluating the impact of wafer bonding on the final performance. We carried out GoG cell characterization under AM1.5 irradiation and for various operating temperatures and solar light concentrations.

2. Fabrication

We prepared Ge-on-Glass cells in six steps, schematically summarized in Fig. 1: (a) growth of a Ge epilayer on a Ge substrate, (b) H-implantation, (c) wafer bonding to glass, (d) layer-splitting and chemical etch-back, (e) growth of the solar element, (f) mesa definition and contact lithography.

#179572 - $15.00 USD Received 8 Nov 2012; revised 21 Dec 2012; accepted 9 Jan 2013; published 10 Jan 2013
(C) 2013 OSA

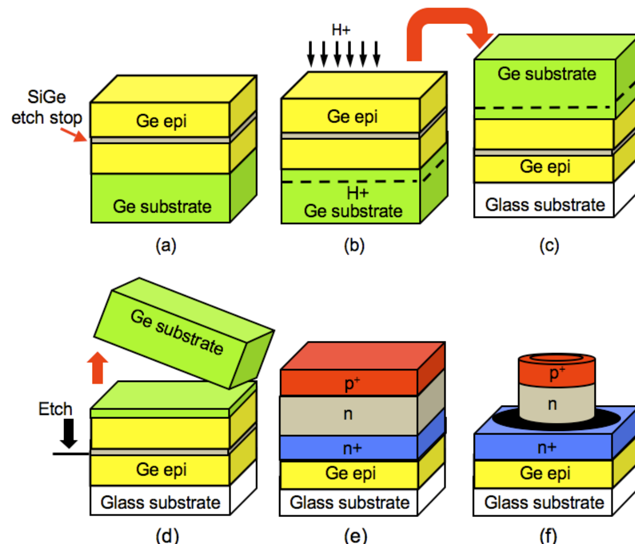

Fig. 1. Process flow of GoG cell fabrication.

A single etch-stop structure (SES) was grown on a 450 µm thick Ge (100) substrate at 550°C and a reduced pressure of 100 mbar, using an ASM Epsilon 2000 CVD reactor. The SES includes a 100 nm Ge buffer layer, a 15 nm 70% SiGe etch-stop and a 50 nm Ge cap layer. The SiGe provides the stop-layer for a chemically selective etch that, following layer transfer, is used to recover a smooth surface suitable for further epitaxial growth. The Germanium cap layer forms the basis of the transferred film. The SiGe film has to be sufficiently thin to remain fully strained and lattice matched to the underlying substrate, but thick enough to form a robust barrier and allow the selective removal of Ge from above whilst protecting the underlying Ge from being etched.

Hydrogen was implanted into the SES structure, on-axis, to a depth of approximately 400 nm below the wafer surface. A dose of H^+ greater than $3 \cdot 10^{16}$ cm^{-2} was found necessary to achieve layer splitting in Germanium [29]. For wafer bonding we chose a commercially available glass (Schott D263T) with thermal expansion coefficient matching that of Ge in the temperature range of the subsequent process (≈550°C). By atomic force microscopy (AFM) we determined a surface roughness of 2Å, pinpointing a good compatibility with direct bonding. This glass proved to be chemically very robust, permitting a thorough chemical cleaning. Both SES and glass were cleaned in a Piranha Etch to eliminate organic contaminants and in RCA SC-1 to remove any residues [30]. The surfaces were prepared for direct bonding by providing an -OH terminated surface to enhance Van der Waals forces. Upon heating, condensation of Van der Waals bonds occurs and give rise to extremely strong covalent bonds with an accompanying loss of H_2O [31].

To form an –OH terminated surface, the glass substrate and the SES structure were treated with NH_4OH diluted with deionized water, rinsed and spun dry without further water exposure. Following the chemical preparation, the two surfaces were aligned, placed in contact and then heated to about 370°C. Finally, the layers were carefully separated, leaving the donor Ge substrate to be reused after recovery by chemi-mechanical polishing.

The surface of the as-cut Ge on glass was too rough and disordered for epitaxial growth; hence, it needed the removal of the damaged layer. Thereby, Ge was etched, selectively removing the disordered portion down to the buried SiGe etch-stop. AFM showed that the etched surface had an rms roughness of around 2 Å. The remaining transferred Ge thin-film on glass was thin enough (60 nm) to be transparent to the eye.

The most challenging obstacle to the re-growth on the GoG platform is the maximum temperature, around 600°C, at which the sample can be processed due to presence of the

#179572 - $15.00 USD Received 8 Nov 2012; revised 21 Dec 2012; accepted 9 Jan 2013; published 10 Jan 2013
(C) 2013 OSA

glass. This limit makes it impossible to prepare a clean surface (suitable for epitaxy) via the standard in situ pre-deposition bake in Hydrogen, as the bake is not effective below 700°C. Therefore, first we chemically removed the surface oxide with both HF and HBr, then, performed a low-temperature in situ bake to remove any remaining volatile species.

We fabricated a simple individual photovoltaic cell on the GoG platform at 550°C and a reduced pressure of 100 mbar. The re-growth was initiated using a Ge tetrachloride precursor ($GeCl_4$), which is better suited for initiating a crystalline re-growth (after the chemical treatment) than the standard Germane (GeH_4) precursor used for the remainder of the structure.

The highly p-type doped back-contact region was grown to a thickness of 1800 nm. To simplify the device processing at a later stage, a 15 nm 75% SiGe etch-stop layer was introduced above the back-contact region. A low p-type doped base region, 2200 nm thick, was deposited and followed by a highly n-type doped emitter, 200 nm thick, on the top of the structure. The doping was carried out by either diborane (B_2H_6) or phosphine (PH_3) for *p* or *n* regions, respectively. The wafer was unloaded after slowly cooling down to 200°C, in order to avoid deformations of the glass substrate. The device fabrication was completed by selectively etching mesas of various areas (between 0.012 and 0.16 cm^2) down to the highly-doped back-contact (by means of the second etch-stop); Aluminum contacts were realized by thermal evaporation and standard lithography.

Figure 2 shows photographs of the GoG platform, a GoG solar cell wafer and a typical wafer comprising several cells. Similar solar structures were fabricated on Ge substrates for comparison.

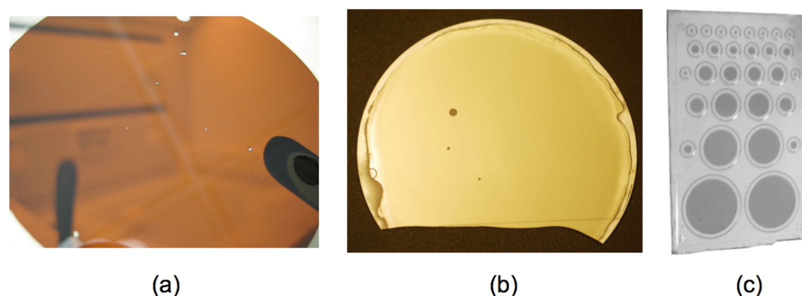

Fig. 2. GoG platform (a), GoG solar cell wafer (b), typical sample comprising several cells (c).

3. Results and discussion

3.1 Material characterization

The completed GoG structures were thoroughly characterized before device fabrication. The wafers were nearly completely covered by Ge, except for the borders where a few holes were visible (Fig. 3). The presence of holes is attributed to particulates trapped between the two surfaces, causing voids in the bonding area. During the pre-growth oxide removal, the presence of microscopic holes allows HF to penetrate and under-etch the bonded material with a consequent increase of the hole size. Careful cleaning procedure before bonding would minimize the problem. However, fully functional devices can be obtained when such holes are avoided during mask-alignment.

Bright light microscope inspection revealed an uneven haze across the wafer surface (haziest at the edge, lightly hazed near the center, shiny in between). Nomarski-type optical inspection confirmed the presence of large pits towards the edge, smaller ones at the center and a few small pits midway in between. We suggest that these surface pits result from incomplete oxide removal from the wafer surface preventing (or delaying) growth in isolated regions. The combination of HBr and HF was quite effective in reducing the hole size on most of the wafer.

#179572 - $15.00 USD Received 8 Nov 2012; revised 21 Dec 2012; accepted 9 Jan 2013; published 10 Jan 2013
(C) 2013 OSA

AFM was used to determine the orientation of the large surface features and also to measure the RMS background surface roughness in the absence of depressions. The RMS surface roughness results were limited to about 0.2 nm, while the depth of the surface depressions across the wafer varied between 100 and 300 nm.

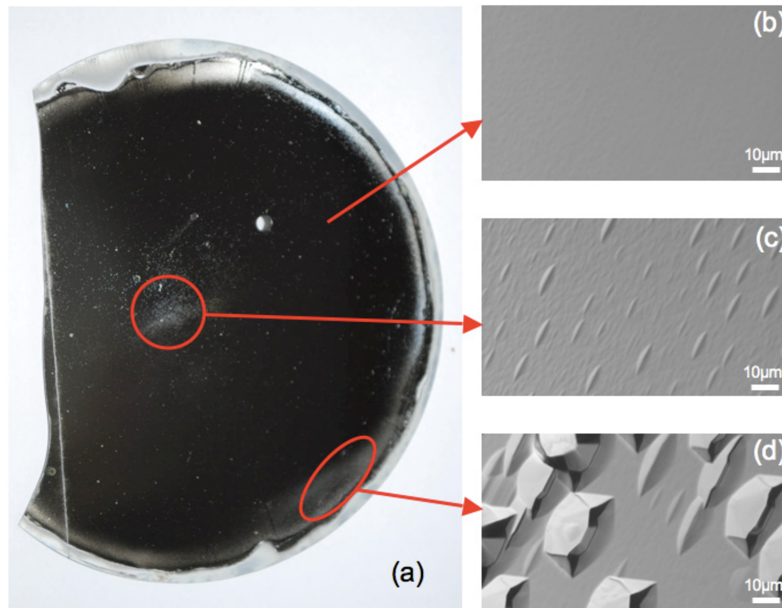

Fig. 3. Photograph of (a) a GoG wafer and zoomed-in images of specific portions: (b) majority of the wafer area, (c) center portion, (d) edge portion.

Transmission Electron Microscopy (TEM) was used to rule out the presence of high densities of threading dislocation defects and to inspect the bonded interface between glass and Germanium for voids. Figure 4 shows a typical result: no dislocations are visible threading to the surface, suggesting a threading dislocation density well below 10^7 cm^{-2}. Larger magnification TEM, however, reveals the presence of dislocations in the bonded Ge layer despite the fact that it is under the critical thickness [32]. Nevertheless, such dislocations did not keep propagating through the re-grown layer. The examination of the diffraction pattern (shown in the inset) obtained from the re-grown Ge clearly indicates it is crystalline: no halos are present to suggest polycrystalline material.

In solar cell applications, it is of paramount importance that the threading dislocation density (TDD) is below 10^6 cm^{-2} [33,34]; therefore, to ensure that the performance of a solar device manufactured on the GoG platform did not degrade, we also performed etch-pit counts to determine the effective TDD. An Iodine etchant was used to selectively etch the Ge surface and reveal threading dislocations as etch pits [35]. The measured typical TDDs (before the emitter fabrication) were 2 to $3{\cdot}10^4$ cm^{-2}. Although we were not able to determine at what stage such TD density occurred, it may be the result of thermal mismatch. Nonetheless, this TDD value can be considered acceptably low for solar cell operation.

#179572 - $15.00 USD Received 8 Nov 2012; revised 21 Dec 2012; accepted 9 Jan 2013; published 10 Jan 2013
(C) 2013 OSA

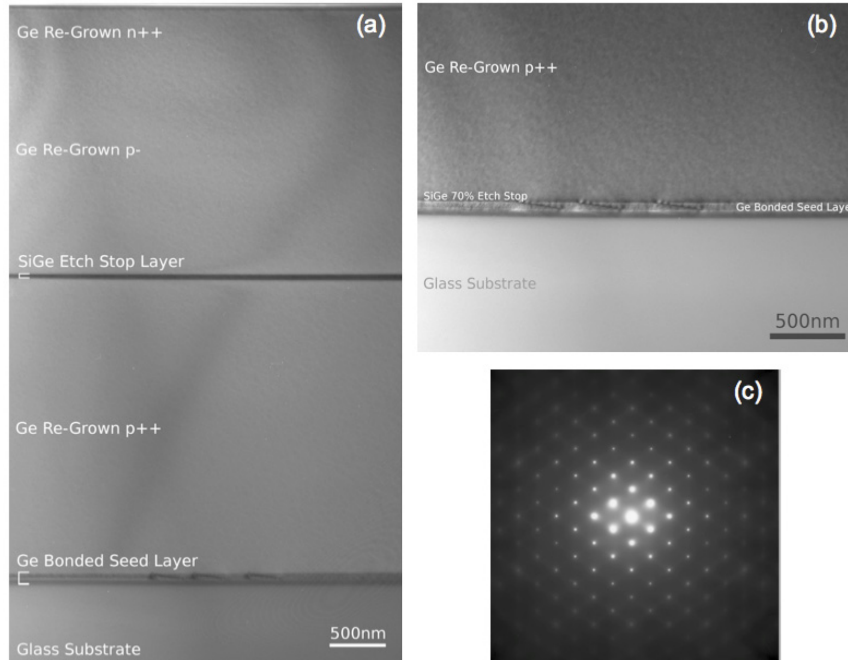

Fig. 4. (a) Cross section TEM of a GOG sample, (b) enlargement of the glass-Ge interface, (c) diffraction pattern.

Finally, secondary ion mass spectroscopy (SIMS) was used to determine the concentration and the distribution of both Boron and Phosphorous in the sample. Figure 5 displays typical results. The doping profiles are abrupt and flat, with a Phosphorous concentration of $6{\cdot}10^{18}$ cm^{-3} in the emitter, a Boron concentration of 10^{17} cm^{-3} in the base and $1.2{\cdot}10^{19}$ cm^{-3} in the bottom contact, respectively. The electrochemical CV profiling confirmed that the dopant activation is close to 100%.

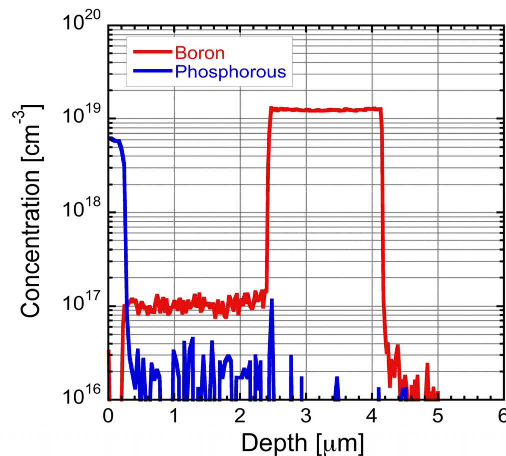

Fig. 5. SIMS showing B and P concentration profiles.

3.2 Solar cell characterization

We performed the cell characterization in two steps: first, we compared GoG and reference Ge-on-Ge cells in order to evaluate the impact of wafer bonding on their final performance;

then, we carried out an extensive characterization of GoG cells under standard AM1.5 illumination and various operating conditions such as temperature and solar concentration. We have adopted a commercial solar simulator (ASTM standard) provided with a Xenon arc lamp and an air mass 1.5 global filter. Characterizations have been performed at 1000W/cm^2 and 25°C. The reference is a monocrystalline silicon cell calibrated and certified against an NREL secondary cell. Except the characterization versus temperature, all measurements have been performed at 25°C. The cells were characterized in terms of dark current density J_d at different reverse biases, ideality factor n and series resistance R_s. They were tested under illumination to measure the short-circuit current density J_{sc}, the open-circuit voltage V_{oc}, the fill factor FF and the energy conversion efficiency η.

Typical results for Ge-on-Glass and test Ge-on-Ge cells are summarized in Table 1, and the best sample characteristics are displayed in Fig. 6. The dark current density at a reverse bias of −1V (a standard figure to assess the quality of Ge epilayers [36]) was remarkably low, with values of about 0.2 and 0.25mA/cm^2 for Ge-on-Ge and GoG, respectively.

Table 1. Performance of Ge-on-Ge and GoG samples (area = 0.088cm^2, T = 25°C, I = 100mW/cm^2)

Parameter	Symbol	Ge on Ge	GoG
Short circuit current density	J_{sc}	23 mA/cm^2	28 mA/cm^2
Open circuit voltage	V_{oc}	144 mV	131 mV
Fill factor	FF	54%	53%
Dark current density @ −1V	J_d	0.2 mA/cm^2	0.25 mA/cm^2
Ideality factor	n	1.08	1.08
Series resistance	R_s	18 mΩcm^2	36 mΩcm^2
Energy conversion efficiency	η	2.1%	1.9%

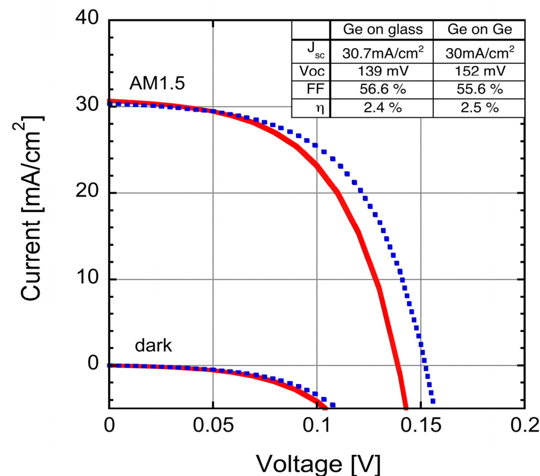

Fig. 6. *I-V* characteristics of the best cells (highest conversion efficiency) in dark and under AM1.5. GoG (red solid lines) and test Ge-on-Ge (blue dotted lines) cells are compared. The corresponding relevant parameters are summarized in the inset. The area of the cells is 0.088cm^2.

By fitting the current-voltage characteristics, we could evaluate an average series resistance of 36 mΩcm^2 for GoG and about half this value for test cells because of their thick substrate. The ideality factor n = 1.08 was the same for the two types.

#179572 - $15.00 USD Received 8 Nov 2012; revised 21 Dec 2012; accepted 9 Jan 2013; published 10 Jan 2013
(C) 2013 OSA

Under AM1.5 illumination we observed a slightly larger J_{sc} with a correspondingly smaller V_{oc} in GoG as compared to Ge-on-Ge samples. Typical J_{sc} and V_{oc} for GoG were 28 mA/cm^2 and 131 mV, respectively, with corresponding values of 26 mA/cm^2 and 144 mV for Ge-on-Ge. The larger V_{oc} of Ge-on-Ge cells is consistent with the lower inverse saturation current, while the larger J_{sc} of GoG cells is due to the reflecting glass substrate. The average fill factor was 53% in GoG and 54% in Ge-on-Ge, respectively.

GoG and Ge-on-Ge cells exhibited average conversion efficiencies close to 1.9 and 2.1%, respectively. Figure 6 shows the *I-V* characteristics of the most efficient samples in dark and under illumination, along with their relevant parameters. The best GoG cell exhibited an energy conversion efficiency as large as 2.4%, close to the 2.5% measured in the best Ge-on-Ge. Thus, since the conversion efficiencies are comparable, we can conclude that the processes of lift-off, bonding and layer splitting do not affect significantly the final performance of GoG with respect to cells grown on their native substrate.

A second set of GoG devices was prepared for a more extensive characterization which included external quantum efficiency and *I-V* characteristics for the extraction of relevant parameters versus device area, operating temperature and solar concentration. Figures 7 and 8 display the *I-V* characteristic and the external quantum efficiency (EQE) of the best sample.

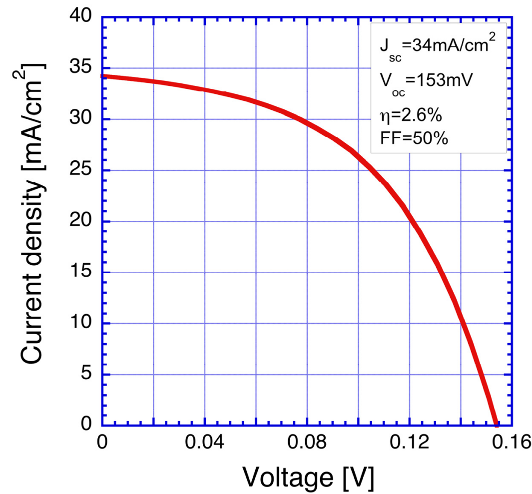

Fig. 7. AM1.5 characteristics of the GoG cell with highest conversion efficiency. The area of the cell is 0.03cm^2.

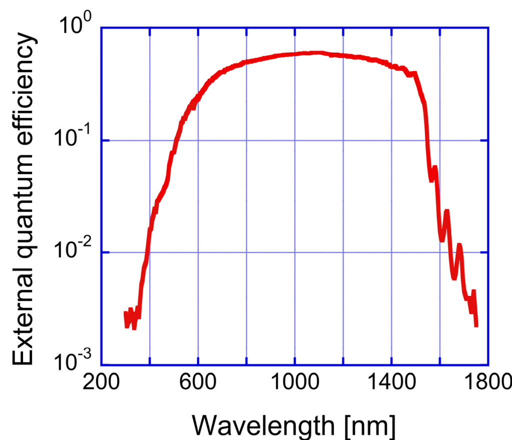

Fig. 8. External quantum efficiency of the most efficient GoG cell.

The slightly better performance with respect to the previous set is due to minor improvements in device processing. The maximum conversion efficiency of 2.6% is quite encouraging, despite being well below the 7.8% record efficiency reported in traditional Ge solar cells [19]. However, it should be considered that the latter value was obtained using 170µm-thick Ge-substrates and an optimized design including anti-reflection coating, passivation and back-surface field. Most of the difference in efficiency is due to the thin absorbing layer (base) of only 2.3 µm in our device. In order to investigate the cell response versus wavelength, we measured the EQE in the range 1.0-1.8 µm, as graphed in Fig. 8. Away from the shortest wavelengths, where the device is not intended to be operated as a bottom cell, the EQE is close to the theoretical maximum calculated assuming a complete carrier collection and using optical absorption values from the literature [37]. At wavelengths above 1350nm the measured EQE starts departing from the expected value: for instance, measured and calculated EQEs are 0.47 and 0.51 at 1380nm, 0.31 and 0.42 at 1512nm, respectively.

Therefore, light that penetrates deeper in the cell is less effectively converted. Since the depletion width of the junction (where complete carrier collection can be assumed) is about 100nm, the EQE values suggest that the diffusion length of minority carriers is shorter than the base length (2.3µm). It follows that the cell performance could be bettered by using thicker films as well as by improving the material quality.

While the material analysis did not provide evidence of large defect density, the optical inspection showed several spots where Ge did not completely nucleate during regrowth (Fig. 3). In order to study the effect of such macroscopic (low density) defects, we measured the efficiency and the V_{oc} of cells with areas in the range 0.012-0.16 cm^2. The results in Fig. 9 suggest that the performance is not affected by such voids, otherwise the efficiency would decrease with the area. On the other hand, a reduction of both V_{oc} and η is observed in small cells, suggesting they undergo edge effects associated to the increase of the perimeter to area ratio. This is confirmed by the measured saturation current, which scales with area in large devices but with perimeter in small devices (graph not shown).

We also investigated the cell operation versus operating temperature, as shown for the relative V_{oc} and η changes in Fig. 10 versus temperature in the interval 25-70°C: the conversion efficiency decreases at about 1.8%/°C. While there is a small photocurrent increase (owing to a small increase in diffusion length and to band-gap narrowing), the dominant change relates to Voc due to the exponential dependence of the saturation current from temperature. The measured $dV_{oc}/dT = -1.9$mV/°C is in good agreement with the theoretical prediction of −1.88mV/°C [38].

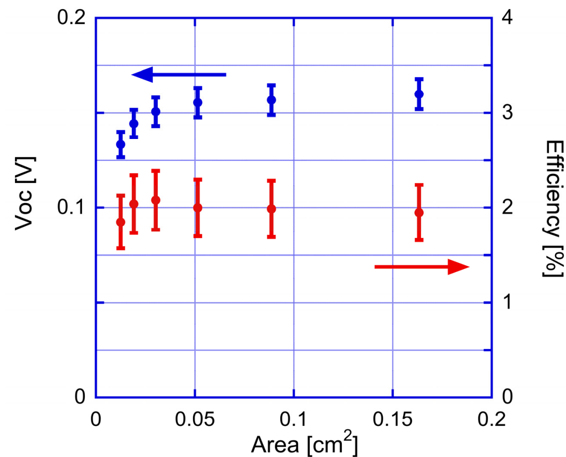

Fig. 9. GoG open circuit voltage (blue) and conversion efficiency (red) versus cell area.

Since GoG cells are mainly intended as bottom elements of multi-junction devices to be operated at high solar concentrations, we also carried out their I/V characterization while

#179572 - $15.00 USD Received 8 Nov 2012; revised 21 Dec 2012; accepted 9 Jan 2013; published 10 Jan 2013
(C) 2013 OSA

increasing the power density from 1 to about 13 suns (Fig. 11) and extracted the corresponding V_{oc}, I_{sc}, η and FF (Figs. 12 and 13). The irradiance corresponding to 1-sun is $100 mW/cm^2$. Irradiance at higher concentrations have been measured by the reference cell.

Although such figures cannot give quantitative data on how the GoG cells will behave when embedded in a multiple cell, the characterization provides interesting information.

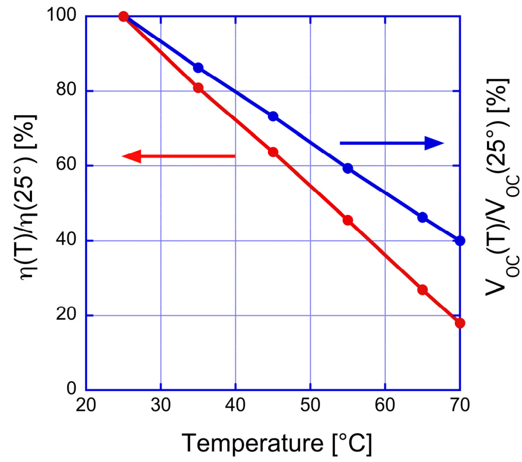

Fig. 10. GoG relative change of efficiency (red) and open circuit voltage (blue) versus temperature.

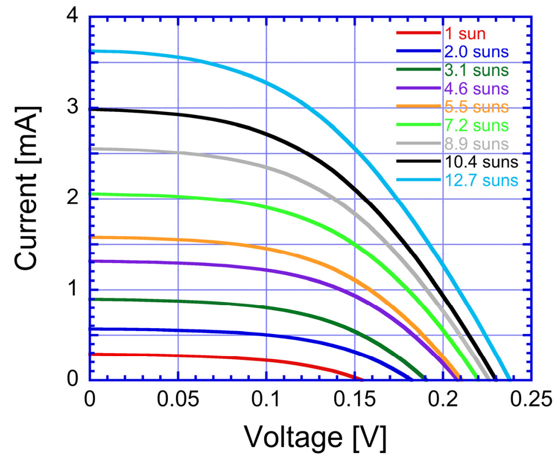

Fig. 11. GoG I-V characteristics for various solar irradiation, from 1 to 12.7 suns.

#179572 - $15.00 USD Received 8 Nov 2012; revised 21 Dec 2012; accepted 9 Jan 2013; published 10 Jan 2013
(C) 2013 OSA

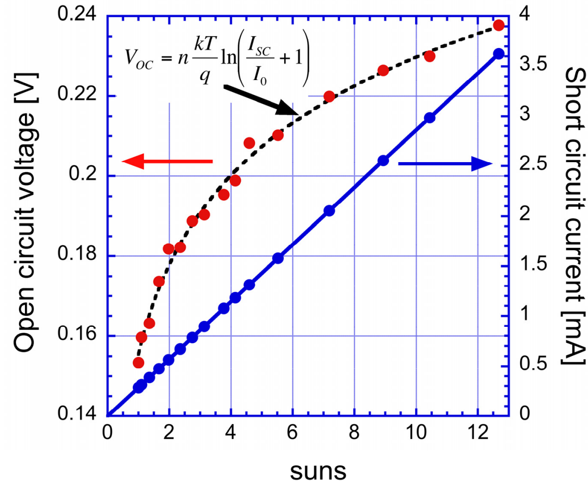

Fig. 12. GoG open circuit voltage and short circuit current for irradiation from 1 to 12.7 suns.

Figure 12 graphs the short circuit current I_{sc} and open circuit voltage V_{oc} versus irradiation: the linearity of I_{sc} versus irradiation and the V_{oc} increase consistent with the ideal diode characteristic (equation in the inset) indicate no cell degradation under intense illumination.

Figure 13 plots the conversion efficiency η and the fill-factor *FF* versus irradiation: while the *FF* has a moderate decrease, the conversion efficiency goes from 2.64% at room temperature to a maximum of about 3.77% around 7 suns (corresponding to a relative change $\Delta\eta/\eta = 42\%$). This observed improvement is much larger than the $\Delta\eta/\eta = 16\%$ suggested by a logarithmic scaling with solar concentration. While this fact is worthy of further investigation, we believe it is related to a significant reduction of η at lower concentrations rather than to an anomalous increase at higher concentrations. The reduction may be connected to surface effects on V_{oc}, more relevant in small cells.

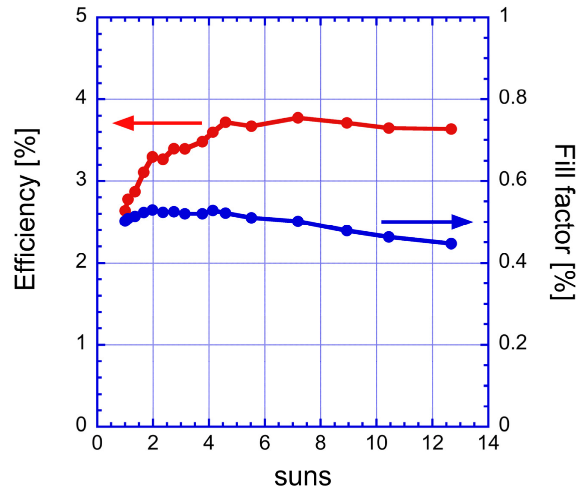

Fig. 13. GoG conversion efficiency (red) and fill factor (blue) versus solar irradiation.

4. Conclusion

In conclusion, we reported and discussed a novel approach for realizing Germanium on glass solar cells based on wafer bonding and epitaxial lift-off followed by epitaxial regrowth. We presented the details of the GoG fabrication and the results of an extensive material

#179572 - $15.00 USD Received 8 Nov 2012; revised 21 Dec 2012; accepted 9 Jan 2013; published 10 Jan 2013
(C) 2013 OSA

characterization, revealing the high quality of the Ge epilayer in terms of both dislocation density and flatness.

The *pn* solar cells fabricated on glass compare well with similar cells epitaxially grown on Ge, demonstrating that the processes of lift-off, bonding and layer splitting do not alter significantly the solar cell and its performance. GoG devices exhibit a very promising maximum conversion efficiency of 2.6% and 3.7% at illuminations of 1 and 8 suns, respectively.

The results of the electrical characterization and their comparison with theoretical predictions indicate that significant improvements are obtainable from thicker optimized GoG structures, making GoG a rather promising and versatile platform towards the production of low-cost bottom elements in multi-junction solar cells.

Acknowledgments

We thank R. Godfrey, C. Meaton and M. Palmer (AdvanceSis) and S. Rampino (CNR-IMEM) for their contribution.

#179572 - $15.00 USD Received 8 Nov 2012; revised 21 Dec 2012; accepted 9 Jan 2013; published 10 Jan 2013
(C) 2013 OSA